JOURNAL OF GEOPHYSICAL RESEARCH, VOL. 102, NO. E5, PAGES 10,933-10,943, MAY 25, 1997

The structure and compensation of the lunar highland crust

Mark A. Wieczorek and Roger J. Phillips

Department of Earth and Planetary Sciences, Washington University, St. Louis, Missouri

Abstract. A new method of interpreting geoid to topography ratios (GTRs) on a sphere is presented, in which it is shown that the GTR is equivalent to a sum of spectrally weighted degree-dependent admittances. Using this method combined with newly obtained gravity, topography, and near-global surface iron concentrations from the Clementine mission, the structure and compensation of the lunar highland crust have been investigated. Geoid to topography ratios were tested against single-layer Pratt and Airy compensation models, as well as dual-layered Airy models. Regional lateral variations in crustal density are found to play an insignificant role in crustal compensation, and the single-layer and dual-layered Airy models both strongly suggest that the lunar crust is vertically stratified. The depth of the intracrustal interface obtained from these models is consistent with the existence of a 20-km seismic discontinuity beneath the Apollo 12 and 14 sites. A uniform density crust with compensation occurring at the Moho is a viable interpretation of crustal structure only when the extreme limits of the observed GTR distribution are used.

Introduction

Perhaps one of the most important discoveries of the Apollo program was that the highland crust of the Moon is anorthositic in composition. Although other rock types have been found at the surface, the manner in which crustal composition varies vertically or laterally has not been well constrained. The volume and distribution of anorthosite have important implications regarding the origin of the crust, the depth of a putative magma ocean, and the bulk composition of the Moon [e.g., *Warren*, 1985]. Using newly acquired data from the Clementine mission, we have used the gravity, topography, and surface iron concentrations to constrain the structure and compensation of the lunar highland crust.

Lunar crustal thickness maps have been constructed traditionally by modeling observed gravity anomalies in terms of variations in surface and Moho relief, the latter of which has been seismically constrained at one location [e.g., *Neumann et al.*, 1996]. Alternatively, it has been proposed by *Solomon* [1978] that the correlation between mineralogy and topography in the Apollo data implies that the crust may be partially compensated by a Pratt mechanism. This suggests that lateral variations in crustal density, as well as crustal thickness variations, may contribute to the lunar gravity field. With the exception of a thin veneer of mare basalt, however, all previous interpretations of the lunar gravity field have assumed inherently that the crust is not compositionally stratified.

Several lines of evidence though do suggest that the crust is in fact vertically stratified. *Ryder and Wood* [1977] and *Charette et al.* [1977] interpreted the noritic low-K Fra Mauro (LKFM) melt rocks [*Reid et al.*, 1972, 1977] as lower crustal material exhumed by basin forming impacts and suggested that the crust was stratified into three zones of distinct mineralogy. In addition, *Spudis et al.* [1984] presented evidence that the composition of basin ejecta becomes more "noritic" with increasing basin size, implying that larger impacts excavate greater amounts of more mafic lower crustal material. More recently, based on a new surface iron concentration map, *Lucey et al.* [1995] interpreted iron concentrations in the South Pole-Aitken (SPA) basin as being representative of LKFM "basalt" and almost certainly lower crustal material. Others, however, have suggested that this basin may represent a mixture of various amounts of basalt, mantle, highland, and lower crustal materials [*Belton et al.*, 1992; *Pieters et al.*, 1993; *Head et al.*, 1993; *Spudis et al.*, 1994; *Lucey et al.*, 1996]. Additional evidence for a stratified crust comes from the Apollo seismic data, which indicates that a seismic discontinuity exists approximately 20 km below the surface in the region of the Apollo 12 and 14 sites [*Toksöz et al.*, 1974]. The interpretation of this discontinuity however is not unique, for it has been proposed to be both compositional in nature and/or an interface between fractured and unfractured rock [*Simmons et al.*, 1973; *Todd et al.*, 1973; *Wang et al.*, 1973; *Toksöz et al.*, 1974].

In order to test the hypothesis that the lunar crust is stratified, we have computed geoid to topography ratios (GTRs) for the highland crust. A new method of interpreting GTRs on a sphere is presented in which we show that the GTR is equivalent to a sum of spectrally-weighted degree-dependent admittances. Using this method, several single and dual-layered Airy compensation models were tested, and it was found that only two of the models examined were consistent with the geophysical and petrological constraints: a single-layer Airy model and a dual-layered Airy model with upper crustal thickness variations and constant thickness lower crust. Both models strongly suggest that the crust is vertically stratified, and the depth of the upper-lower crustal interface obtained from these models is found to be consistent with the observed 20-km seismic discontinuity below the Apollo 12/14 site. Only in the most extreme scenarios is a uniform density crust with compensation occurring at the Moho compatible with the GTRs. Using an empirical relationship between density and iron concentration, we also show that regional lateral variations in crustal density for the highlands are negligible, suggesting that Pratt compensation is unimportant. These results support the view that the 20-km seismic discontinuity is at least partially compositional in nature [*Toksöz et al.*, 1974], and leads to the hypothesis that this boundary is widespread within the lunar crust.

Paper number 97JE00666.
0148-0227/97/97JE-00666$09.00

Spectrally Weighted Admittances

Gravity and topography data can be used to invert for many geophysical parameters, including, but not limited to, the structure and thickness of the crust of a planetary body. Both spectral and spatial techniques have been used to investigate this problem [e.g., *Ockendon and Turcotte,* 1977; *Haxby and Turcotte,* 1978; *Dorman and Lewis,* 1970], each having their separate merits and caveats. Spectral techniques (when applicable) are generally superior in that a wavelength-dependent admittance function can be calculated. The form of the calculated admittance may give hints as to the mechanism causing the gravity and topography anomalies (e.g., crustal thickness variations versus flexure versus convection), and the wavelength-dependent amplitude can often be used to invert for several model parameters. In contrast, most spatial techniques calculate only an admittance that is independent of wavelength, thus discarding any additional spectral information that may be available.

One downfall of spectral techniques is that admittances with wavelengths greater than the size of the region being investigated cannot be obtained. Additionally, one generally wishes to investigate regions that have a uniform mechanism of compensation, for if provinces with disparate compensation mechanisms were included in the analysis, the computed admittance function would then represent an average of these regions [e.g., *Forsyth,* 1985; *Zuber et al.,* 1989]. In practice, these factors often place strict constraints on the size of the region being investigated, and subsequently the range of wavelengths analyzed. As an example, in this study we wish to investigate the compensation of the lunar highlands without including regions which contain extensive mare basalt flows. If a spectral method were used in this case, the largest square region that one could analyze for the lunar nearside would be roughly 1000 km to a side. Since the gravity field is only poorly known at short wavelengths, a spatial approach in this instance is clearly warranted.

As an aside, we mention a new method due to M. Simons et al. (Localization of gravity and topography: Constraints on the tectonics and mantle dynamics of Venus, submitted to *Geophysical Journal International,* 1996) that has been developed to obtain spectral information on a sphere over localized regions. In this method, localized regions are obtained by multiplying the spherical data by a windowing function. The admittance function relating the spherical harmonic coefficients of the localized gravity and topography fields can then be computed and used as a constraint in geophysical models. Though much improved over the traditional Cartesian method of Fourier transforming regional gravity and topography data, this technique suffers from the same caveats as expounded above.

In this section a spatial technique is developed in which GTRs can be used to invert for parameters of a given degree-dependent admittance model. Specifically, we show that the GTR on a sphere is equivalent to a weighted degree-dependent admittance. Furthermore, if the GTR can be shown to be independent of position, then the weighting function is proportional to the power in the topography for each corresponding degree.

The geoid and topographic height for any point on a spherical body is given by

$$\begin{aligned} N(\theta,\phi) &= R\sum_{ilm} C_{ilm}\, Y_{ilm}(\theta,\phi) \\ T(\theta,\phi) &= R\sum_{ilm} h_{ilm}\, Y_{ilm}(\theta,\phi) \end{aligned} \tag{1}$$

where R is the mean planetary radius, C_{ilm} are the potential coefficients, h_{ilm} are the topographic coefficients, $Y_{ilm}(\theta,\phi)$ is the spherical harmonic function, and θ and ϕ are the colatitude and longitude, respectively, in center of mass coordinates. The potential and topography coefficients are related by the linear transfer function (admittance) Z_l:

$$C_{ilm} = Z_l\, h_{ilm}, \tag{2}$$

allowing the GTR for a given point to be expressed by

$$\begin{aligned} \mathrm{GTR}(\theta,\phi) = \frac{N(\theta,\phi)}{T(\theta,\phi)} &= \frac{\sum\limits_{ilm} Z_l\, h_{ilm}\, Y_{ilm}(\theta,\phi)}{\sum\limits_{ilm} h_{ilm}\, Y_{ilm}(\theta,\phi)} \\ &= \sum_{l} Z_l\, W_l(\theta,\phi) \end{aligned} \tag{3}$$

where the weighting function

$$W_l(\theta,\phi) = \frac{\sum\limits_{im} h_{ilm}\, Y_{ilm}(\theta,\phi)}{\sum\limits_{ilm} h_{ilm}\, Y_{ilm}(\theta,\phi)} \tag{4}$$

represents the fractional contribution of the topography for a given degree l to the total topography at position (θ,ϕ).

W_l and the GTR are in general dependent on position. It is likely, however, that when the GTR is averaged over sufficiently large regions, that this regionally averaged value will be globally uniform (assuming a uniform compensation mechanism). We will assume that the GTR is a stationary property and assess this assumption in the following section.

Assuming that the GTR is stationary necessarily implies that W_l is also independent of position. Rewriting equation (4) as

$$W_l \sum_{ilm} h_{ilm}\, Y_{ilm}(\theta,\phi) = \sum_{im} h_{ilm}\, Y_{ilm}(\theta,\phi), \tag{5}$$

multiplying both sides by

$$\sum_{i'l'm'} h_{i'l'm'}\, Y_{i'l'm'}(\theta,\phi), \tag{6}$$

integrating over all space, and utilizing the orthogonality properties of the spherical harmonic functions, W_l reduces to

$$W_l = \frac{\sum\limits_{im} h_{ilm}^2}{\sum\limits_{ilm} h_{ilm}^2}. \tag{7}$$

Defining the dimensionless power spectra V_l^2 [*Kaula,* 1967]

$$V_l^2 = \sum_{im} h_{ilm}^2 \tag{8}$$

the GTR can finally be expressed as

$$\mathrm{GTR} = \sum_{l} W_l\, Z_l \tag{9}$$

where

$$W_l = \frac{V_l^2}{\sum\limits_{l} V_l^2} \tag{10}$$

is the fractional topographic power for degree l. The GTR for a given admittance model can thus be readily calculated if the global topographic field of the planet is known.

Equations (9) and (10) show that the GTR is most heavily weighted by those degrees which contain significant power. Since the power spectra of planetary topography is "red" [e.g., *Bills and Lemoine,* 1995], the GTR will be most heavily weighted by the

lowest degrees and have little or no contribution from the highest degrees. The topographic power spectrum for the Earth, Venus, and Moon closely follows a power law of the form

$$V_l^2 = A\, l^{-\beta} \tag{11}$$

where A and β are constants. This is a consequence of topography being "fractal" [e.g., *Turcotte,* 1987] with β being approximately equal to 2.2 for Earth [*Rapp,* 1989], 1.5 for Venus, and 1.2 for the Moon. Using this power law for the Moon, it is found that admittances with degrees less than 10 make about a 50% cumulative contribution to the GTR, and degrees greater than 30 make only a 20% cumulative contribution.

Isostatic Admittance Models

Three Airy admittance models were tested against the observed lunar GTRs. For each of these models, the condition of isostasy where equal mass lies in vertical columns was used (see Figure 1). For a simple single-layer Airy model, the admittance Z_l and crustal thickness H' at elevation h are given by [e.g., *Lambeck,* 1988]

$$Z_l = \frac{4\pi\rho_u R^3}{M(2l+1)}\left[1 - \left(\frac{R-H}{R}\right)^l\right] \tag{12}$$

and

$$H' = H + h\left[1 + \frac{\rho_u}{\rho_l - \rho_u}\left(\frac{R}{R-H}\right)^2\right] \tag{13}$$

where ρ_u and ρ_l are the density above and below the compensating interface, M is the mass of the planet, and H is the crustal thickness at zero-elevation (see Figure 2 for representative examples of the above and following admittance functions). When this model is applied to the Moon, it is of significant interest to determine whether compensation occurs at the lunar Moho (in which case ρ_u, ρ_l, and H correspond to crustal and mantle densities and zero-elevation crustal thickness respectively), or at an intracrustal density interface (in which case ρ_u, ρ_l, and H correspond to the upper and lower crustal density and zero-elevation upper crustal thickness). Variations in crustal thickness for this model may be due to the redistribution of surface materials by impact processes, or may represent the remnants of primordial "rockbergs" that floated in a magma ocean.

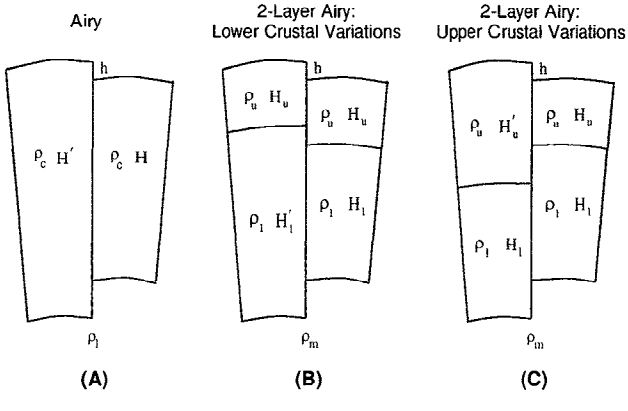

Figure 1. Schematic illustration of single and dual-layered Airy isostatic models: (a) single layer, uniform density crust; (b) constant thickness upper crust, variable thickness lower crust; and (c) variable thickness upper crust, constant thickness lower crust.

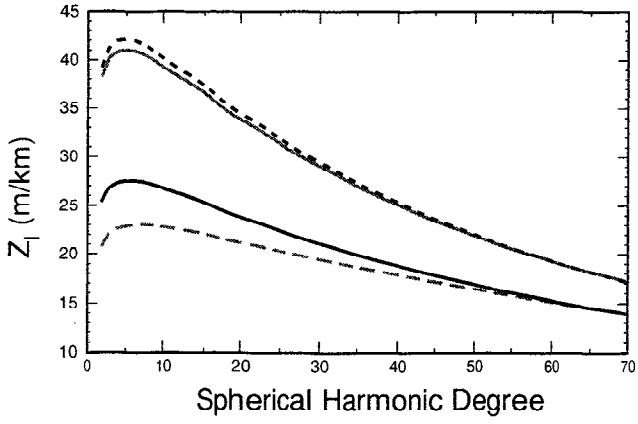

Figure 2. Degree dependent geoid to topography ratios for single-layered and dual-layered Airy compensation models. Upper dotted curve shows dual–layer Airy model with lower crustal thickness variations for $H = 65$ km, $H_u = 25$ km, $\rho_u = 2800$ kg/m^3, $\rho_l = 3100$ kg/m^3, and $\rho_m = 3400$ kg/m^3. Upper solid curve shows single-layer Airy model with $H = 65$ km and $\rho_u = 2900$ kg/m^3. Lower solid curve shows dual–layer Airy model with upper crustal thickness variations for $H = 65$ km, $H_u = 25$ km, $\rho_u = 2800$ kg/m^3, $\rho_l = 3100$ kg/m^3, and $\rho_m = 3400$ kg/m^3. Lower dashed curve shows single-layer Airy model with $H = 35$ km and $\rho_u = 2900$ kg/m^3. Note that the admittance functions for the two dual-layered models are similar to single-layer Airy compensation at either 35 or 65 km depth.

Dual-layered Airy compensation models will be considered in which perfectly rigid "crustal columns" sink isostatically into the lunar mantle. For simplicity, one layer will be allowed to vary in thickness while the other layer remains unchanged (see Figure 1). In practice it will be assumed that the total crustal thickness is known, and the admittance models will be used to solve for the upper crustal thickness.

If lower crustal thickness variations occur with a constant thickness upper crust, the admittance and total crustal thickness are given by

$$Z_l = \frac{4\pi\rho_u R^3}{M(2l+1)}\left\{-\left(\frac{R-H_u}{R}\right)^l\left[1+\frac{\rho_m-\rho_l}{\rho_l-\rho_u}\left(\frac{R-H}{R-H_u}\right)^2\right]^{-1} - \left(\frac{R-H}{R}\right)^l\left[1+\frac{\rho_l-\rho_u}{\rho_m-\rho_l}\left(\frac{R-H_u}{R-H}\right)^2\right]^{-1}+1\right\} \tag{14}$$

and

$$H' = H + h\left[1 + \frac{\rho_u + (\rho_l-\rho_u)\left(\frac{R-H_u}{R}\right)^2}{(\rho_m-\rho_l)\left(\frac{R-H}{R}\right)^2}\right] \tag{15}$$

where H and H_u are the zero-elevation total and upper crustal thickness, respectively. This model may describe a scenario in which the upper portion of the crust has been fractured by impact shock waves to a uniform depth, causing its density to be lower than deeper undisturbed crustal rocks. It may also describe a situation in which the lower crustal thickness varied due to magma ponding at the crust-mantle boundary, and/or to the erosion and redistribution of lower crustal material by vigorous mantle convection.

If variations in upper crustal thickness occur with a constant thickness lower crust, then the admittance and total crustal thick-

ness are accordingly given by

$$Z_l = \frac{4\pi\rho_u R^3}{M(2l+1)}\left\{1+\frac{\rho_l-\rho_u}{\rho_u}\left(\frac{R-H_u}{R}\right)^{l+2} - \left(\frac{R-H}{R}\right)^{l}\left[1+\frac{\rho_l-\rho_u}{\rho_u}\left(\frac{R-H_u}{R}\right)^{2}\right]\right\} \quad (16)$$

and

$$H' = H + h\left[1+\frac{\rho_u}{(\rho_l-\rho_u)\left(\frac{R-H_u}{R}\right)^2+(\rho_m-\rho_l)\left(\frac{R-H}{R}\right)^2}\right]. \quad (17)$$

Upper crustal thickness variations for this model may be due to the redistribution of surface materials caused by basin forming impacts, or may be remnants of primordial rockbergs.

A simple spherical admittance model that linearly relates the potential to the topographic coefficients does not exist for a Pratt compensation model. As an approximation to the GTR, we use

$$\mathrm{GTR} = \frac{\pi\rho_0 R^2 H}{M} \quad (18)$$

from *Haxby and Turcotte* [1978] where ρ_0 is the density at zero-elevation. On a sphere, the density at elevation h is given by

$$\rho = \rho_0\frac{R^3-(R-H)^3}{(R+h)^3-(R-H)^3}. \quad (19)$$

Figure 3 shows plots of the model Airy GTRs as a function of total or upper crustal thickness using the method of spectrally weighted admittances and the known lunar topographic coefficients. Also shown is the GTR predicted from the dipole-moment method of *Ockendon and Turcotte* [1977] and *Haxby and Turcotte* [1978]. As can be seen, the dipole-moment method always overestimates the GTR when compared to the spectrally weighted admittance method for the above Airy models. For the single-layer Airy and two–layer Airy model with upper crustal thickness variations, the dipole-moment method would underestimate the model crustal thickness, whereas for the two-layer model with lower crustal thickness variations, the dipole-moment method would overestimate the upper crustal thickness. It should be noted that the functional relationship between the GTR and H_u for both of the two-layered models are relatively flat. Robust estimates of the upper crustal thickness may not be possible, but the magnitude of the observed GTRs should clearly be able to distinguish between the two models.

Next we empirically assess the assumption that the regionally averaged GTR is independent of position for the above Airy admittance models. To do this, a "synthetic" geoid was computed using the above admittance models and the known lunar topographic coefficients. As discussed in a later section, spherical harmonic degrees 0, 1, and 2 were removed from consideration, and highland geoid and topographic data values within 100, 500, and 1000 km radius circles were regressed to determine the GTR. Figure 4 shows histograms of the computed GTRs for each of the Airy compensation models. As can be seen, for circle radii larger than about 500 km, the synthetic GTRs match the predicted value fairly well. A minor exception is the two-layer model with upper crustal thickness variations which underestimates the actual GTR by about 5 m/km. If the degree 2 terms were left in for the above calculations, the model and predicted GTRs in Figure 4 would only be decreased by about 1 m/km.

Although the average synthetic GTR generally matches the predicted value fairly well when using large data circles, some of the models show more scatter than others. This is related to a breakdown in the assumption that W_l is independent of position, coupled with the fact that some of the admittance functions are strongly degree dependent (see Figure 2). For example, if the admittance was independent of degree, then the GTR would not depend at all on the form of W_l (see Equations (9) and (10)). However, if the admittance was strongly degree dependent, then slight spatial variations in W_l could possibly lead to significant spatial variations in the predicted GTR.

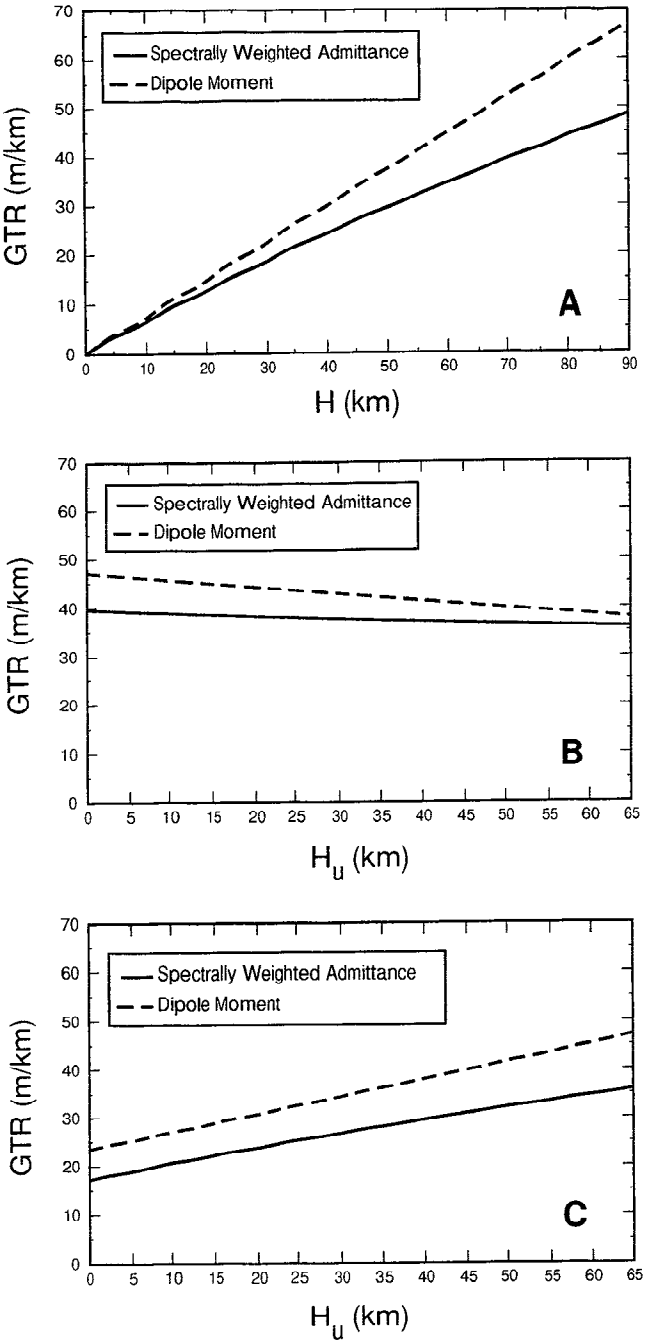

Figure 3. Model GTRs as a function of zero-elevation total or upper crustal thickness. (a) Single layer Airy compensation with $\rho_u = 2900$ kg/m^3. (b) Two-layer Airy compensation with variable thickness lower crust for $\rho_u = 2800$ kg/m^3, $\rho_l = 3100$ kg/m^3, $\rho_m = 3400$ kg/m^3, and $H = 65$ km. (c) Two-layer Airy compensation with variable thickness upper crust for $\rho_u = 2800$ kg/m^3, $\rho_l = 3100$ kg/m^3, $\rho_m = 3400$ kg/m^3, and $H = 65$ km.

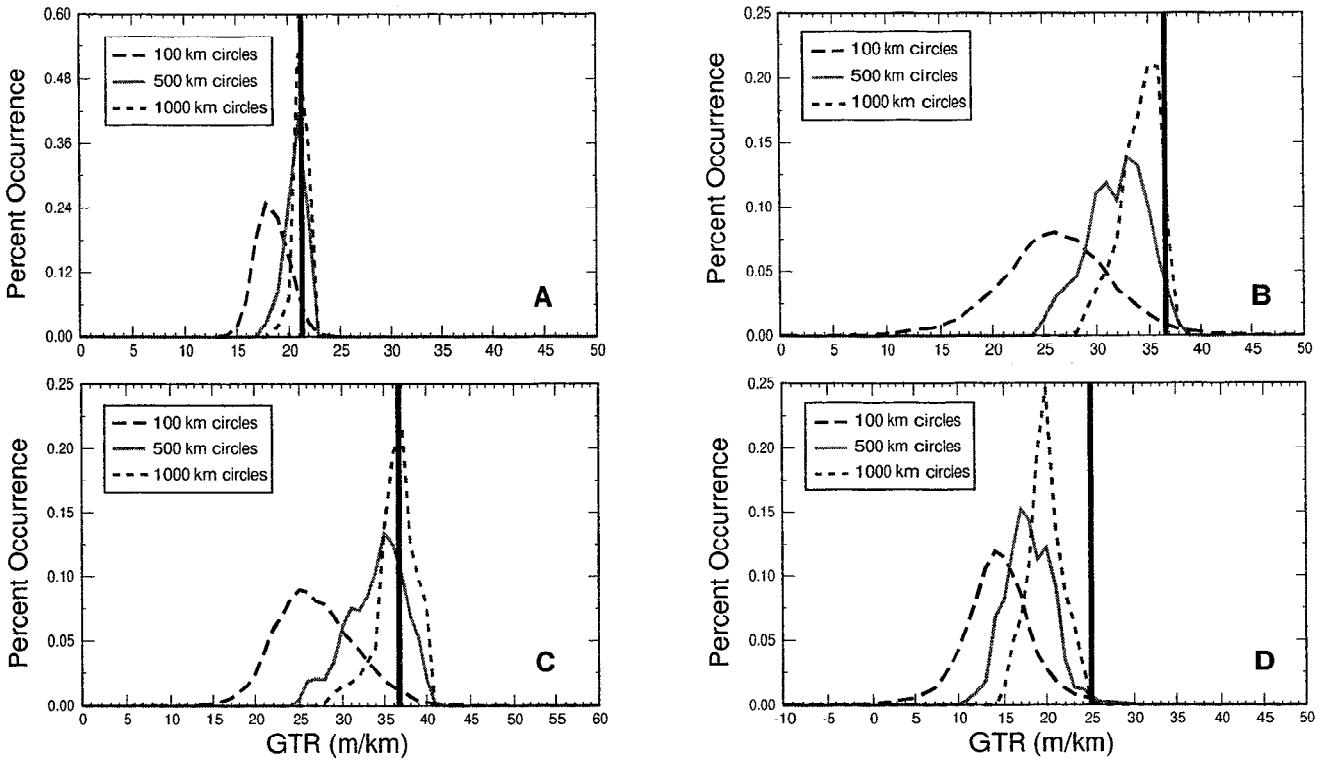

Figure 4. "Synthetic" GTRs computed from the following isostatic admittance models: (a) Single-layer Airy with $\rho_u = 2900$ kg/m^3 and $H = 35$ km. (b) Single-layer Airy with $\rho_u = 2900$ kg/m^3 and $H = 65$ km. (c) Two-layer Airy with lower crustal thickness variations for $\rho_u = 2800$ kg/m^3, $\rho_l = 3100$ kg/m^3, $\rho_m = 3400$ kg/m^3, $H_u = 25$ km, and $H = 65$ km. (d) Two-layer Airy with upper crustal thickness variations for $\rho_u = 2800$ kg/m^3, $\rho_l = 3100$ kg/m^3, $\rho_m = 3400$ kg/m^3, $H_u = 25$ km, and $H = 65$ km. Vertical bar represents the predicted value using the method of spectrally weighted admittances.

Petrological Constraints

All of the above admittance models contain a significant number of parameters, and at first glance may seem significantly underdetermined. In order to obtain meaningful results (enabling one to distinguish between the various compensation models), reasonable constraints must be imposed. In this and the following section we attempt to constrain the mantle density, upper and lower crustal densities, and the total crustal thickness using petrological and seismological arguments.

If the lunar surface abundance of all major rock forming elements were known, the composition and density of the surface materials could be determined by using some appropriate mineralogical norm. The simple mineralogy of the returned lunar highland rocks however allows one to make estimates of composition based on abundances of only a few major elements such as Fe, Mg, and Ti, which were obtained from the Apollo gamma ray experiment [*Bielefeld et al.*, 1976; *Metzger and Parker*, 1979]. Assuming that the minerals anorthite, enstatite, ferrosilite, fayalite, forsterite, and ilmenite dominate the composition of the lunar highland crust, *Haines and Metzger* [1980] calculated the densities of various highland regions using an assumed pyroxene to olivine ratio of 3. It was found that the calculated densities depended only slightly on this ratio and that the addition of any clinopyroxenes in the calculation had a negligible effect. Following *Solomon* [1978] and *Haines and Metzger* [1980], we take the major element surface chemistry as being representative of the upper portion of the underlying crust.

Since the gamma ray data are only available along the Apollo 15 and 16 Command and Service Module ground tracks, it would be advantageous to use the near-global iron concentration map of *Lucey et al.* [1995] to constrain crustal density over a larger region. Densities from *Haines and Metzger* [1980] are plotted versus iron weight percent in Figure 5 and are seen to be highly correlated. Included in this fit are four data values from the Van de Graaff region which is located in the northern portion of the South Pole-Aitken (SPA) basin. Using this empirical relationship between iron and density coupled with the near-global iron concentration map, the density of the lunar crust can be estimated.

Before the density of highland regions can be calculated, however, it is necessary to have a criteria for distinguishing between the highland, mare, and SPA basin terrains. Although this could

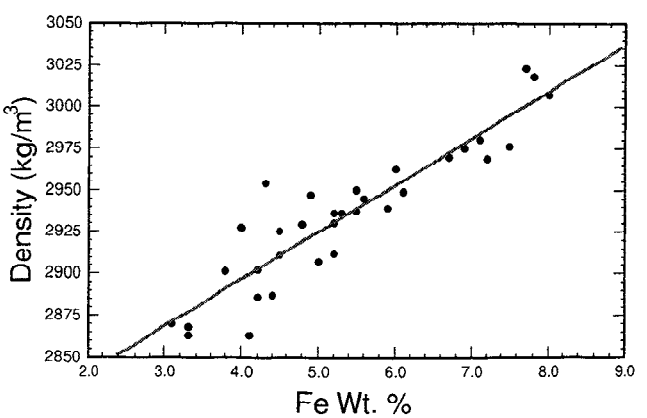

Figure 5. Plot of density versus iron wt % for data from *Haines and Metzger* [1980]. Best fit line is given by $\rho = (2784 \pm 12) + (28.1 \pm 2.2)$ Fe wt % with $R = 0.9168$. A similar relationship is obtained if data from *Solomon* [1978] are used.

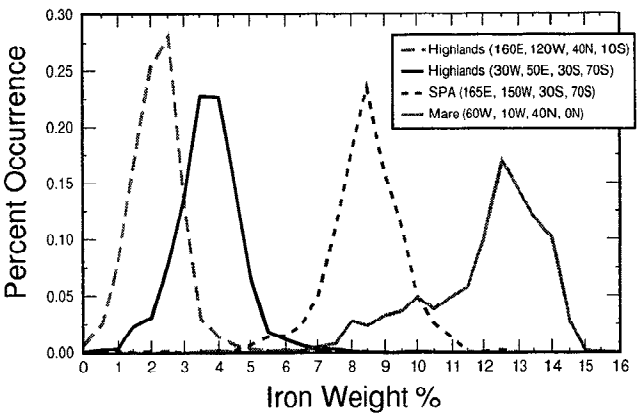

Figure 6. Relative abundance of iron in "typical" nearside and farside highland, South Pole-Aitken, and mare terrains.

be done by "eye" or by using some topographic constraint, the iron abundance turns out to be a fairly robust indicator of terrain type. Figure 6 shows the relative abundance of iron for typical regions of each of these terrains. The highlands in general have iron abundances less than 5.5 wt % while the mare and SPA basin have abundances greater than this. Using this value as a cutoff between the highlands and more mafic units, the average density of the nearside and farside highlands are computed to be 2885 and 2856 kg/m^3, respectively. Although this asymmetry in highland iron abundances and density may be real (and hence contribute to the lunar center-of-mass/center-of-figure offset), it is likely that the nearside highlands are contaminated by greater amounts of mare basalt. A thinner nearside crust would also tend to increase the surface iron abundance by facilitating the excavation of more mafic lower crustal materials.

These highland density values are valid only for unfractured rocks. Microfractures formed by impact shock waves will tend to decrease the density computed from a mineralogic norm, as well as effect elastic properties such as the seismic velocity [e.g., *Simmons et al.*, 1975]. Density models of the Ries impact crater provide an estimate of the magnitude of this effect. Using Bouguer gravity anomalies combined with seismic profiles it has been determined that density anomalies beneath the crater floor exist to a depth of 6 km (equivalent pressures on the Moon are obtained at 36 km depth) with an average negative anomaly of about 125 kg/m^3 [*Pohl et al.*, 1977]. This corresponds to a 5% decrease in density. Using this value, we constrain the density of the upper highland crust to lie between 2885 and 2710 kg/m^3.

Following the suggestion of *Lucey et al.* [1995], we will assume that the SPA impactor excavated lower crustal material. The regolith in this basin will then be composed of a mixture of highly feldspathic highland rocks and more mafic lower crustal material. We take the maximum iron abundance of this region (12.7 wt %) as being the least contaminated by highland rocks, and therefore likely to be representative of pristine lower crustal material. Using newly obtained titanium concentrations from the Clementine mission combined with the iron data, *Lucey et al.* [1996] have recently suggested that the regolith of this basin may represent a 50/50 mixture of lower crustal LKFM and mantle material. As a lower bound on the lower crustal iron concentration, we exclude 50% of the highest iron concentrations in this basin to obtain a value of 8.3 wt %. Extrapolating the linear relationship of Figure 5 gives upper and lower bounds for the lower crustal density of 3140 and 3020 kg/m^3, respectively. Though perhaps fortuitously, this density range compares favorably with the values of 3100 and 3050 kg/m^3 which were suggested by *Ryder and Wood* [1977] for lower crustal LKFM and norite-troctolite rich layers.

Seismological Constraints

The Apollo seismic experiment obtained information on the seismic velocity structure below the Apollo 12, 14, 15, and 16 sites [*Toksöz et al.*, 1974; *Goins et al.*, 1981]. Beneath the Apollo 12/14 mare site, seismic discontinuities were observed at approximately 20 and 60 km. Velocities were found to continually increase from the surface to a depth of 20 km, at which point a jump in velocity occurred, while from 20 to 60 km the velocities remained relatively constant. The highland site of Apollo 16 has been investigated by *Goins et al.* [1981] and was found tentatively to have discontinuities occurring at 20 and 75 km.

While the 60–km and 75–km discontinuities have traditionally been interpreted as the lunar Moho, there is no consensus on the nature of the 20–km discontinuity. *Liebermann and Ringwood* [1976] claim that seismic velocities alone cannot distinguish between rocks of gabbroic, anorthositic gabbro, or anorthositic composition, thus the composition of material below this interface cannot be seismically inferred. Many, however, have interpreted the increasing velocities with depth of the upper crust as attributable to the closure of impact shock-induced fractures, while the constant velocities of the lower crust have been suggested to be representative of unfractured rock [*Simmons et al.*, 1973; *Todd et al.*, 1973; *Wang et al.*, 1973]. Lithostatic pressures alone at 20 km depth however are not sufficient to close all fractures, in fact some fractures should remain open even at 60 km depth. Additionally, if microfractures were annealed due to the higher temperatures at depth, the seismic velocity would be expected to vary smoothly and not to form a jump discontinuity. A purely fracture origin of this discontinuity thus seems unlikely. As was originally suggested by *Toksöz et al.* [1974], the jump in seismic velocity at 20 km depth combined with the above considerations suggests that this interface may represent both a change in composition as well as an interface between fractured and unfractured rocks.

Determining the nature of the 20–km discontinuity is of prime importance. To test whether the depth of this boundary is constant (as was suggested by *Goins et al.* [1981]) or varies laterally, the total zero-elevation crustal thickness for the two-layer Airy models needs to be constrained. We use the seismically obtained crustal thickness of 60 km at the Apollo 12/14 mare site as a reference, and assume that the difference in elevation from mean planetary radius for this site is compensated. A major part of this paper is to determine whether a 20–km density contrast at either the highland or mare site is compatible with the isostatic geoid models.

The last constraint to be imposed on these models is the density of the upper mantle. This value can be constrained by using the Apollo seismic results in conjunction with the observed lunar moment of inertia. All of these models suffer from rather fundamental uncertainties ranging from the existence and size of the lunar core to the nature of the relationship between temperature and depth. Moment of inertia studies though prohibit the upper mantle density from being any larger than 3510 kg/m^3 [*Bills and Rubincam*, 1995], and unlikely to be any lower than 3320 kg/m^3 if a large core is present [*Toksöz et al.*, 1974]. A more realistic upper bound of 3430 kg/m^3, which is consistent with the seismic data, will be used [*Hood*, 1986; *Mueller et al.*, 1988].

GTR Calculations

The 70th degree and order lunar topography (GLTM-2b) [*Smith et al.*, 1997] and gravitational-potential models (GLGM-2) [F. G. Lemoine et al., GLGM2: A 70th degree and order lunar gravity model from Clementine and historical data, *submitted to J. Geophys. Res.*, 1996] obtained from the Clementine mission [*Nozette et al.*, 1994; *Zuber et al.*, 1994] were used to calculate geoid to topography ratios for the lunar highlands. The entire topographic and potential field obtained from the spherical harmonic models were used with three exceptions: (1) Elevations were referenced to mean planetary radius (i.e., the degree 0 topography term was removed). (2) The degree 1 topography terms were removed since there is no associated potential anomaly in center-of-mass coordinates. The degree 1 terms may be a consequence of hemispheric crustal thickness variations [e.g., *Lingenfelter and Schubert*, 1973; *Haines and Metzger*, 1980] or possibly density variations within the crust or mantle [e.g., *Wasson and Warren*, 1980]. (3) The C_{22} and J_2 terms were removed from both fields since these terms are most likely dominated by "fossil" tidal and rotational flattening from an early stage in lunar history [e.g., *Lambeck and Pullan*, 1980]. As justification, we note that the hydrostatic flattening corresponding to the present rotation rate is negligible. In addition, if the entire topographic J_2 were compensated, the associated potential anomaly could only account for at most 20% of the present potential J_2. We additionally remove the remaining degree 2 terms, for if the orientation of the Moon changed after acquiring a fossil bulge [*Melosh*, 1975] these terms would have also become biased.

The first step in computing highland GTRs was to set up an equidistant grid from which geoid and topography data values would be used. As a guide to the spacing between grid points, we assumed that the roughly 5000 potential coefficients corresponded to nearside gravity "measurements," and that these measurements were uniformly spaced, giving a grid spacing of about 60 km (or 2 degrees latitude and longitude at the equator). We note that 60 km is also roughly the half-wavelength of the largest degree in the potential and topographic spherical harmonic models. For each point on this grid, a linear least squares fit between the geoid and topography was obtained for data points within 500, 750, and 1000 km radius circles having iron concentrations less than 5.5 wt %. The GTR was set to zero if more than half of the data points within a given circle were rejected or if the resulting regression had more than a 1% probability of being uncorrelated. Since the uncertainty in the farside geoid is substantially larger than the nearside over broad regions, we only report results for the nearside highlands. The inclusion of farside data however would not significantly alter our conclusions.

The GTRs were found to be independent of the grid spacing, and the uncertainty in the regression for each point was typically less than 3 m/km. The standard deviation of the geoid from the least squares fit was between 20 and 60 m, or nearly 3 times the formal geoid error obtained from the potential covariance matrix. Plate 1 shows an image of the highland GTRs, and Figure 7 shows a histogram of the nearside GTRs. It can be seen that the nearside GTRs are fairly uniform and are independent of the circle radius that was used to collect the geoid and topography data values. In the following section we test the various compensation models using the 1σ limits of the nearside GTR distribution for the case where 1000 km radius circles were used (24 ± 10 m/km).

Results

Although GTRs were only computed for the highlands, crustal thickness estimates for mare sites may be obtained by extrapolating the highland results under an isostatic assumption. In doing so, one must accommodate for the thickness of mare fill, which may either be compensated or uncompensated. However, for the

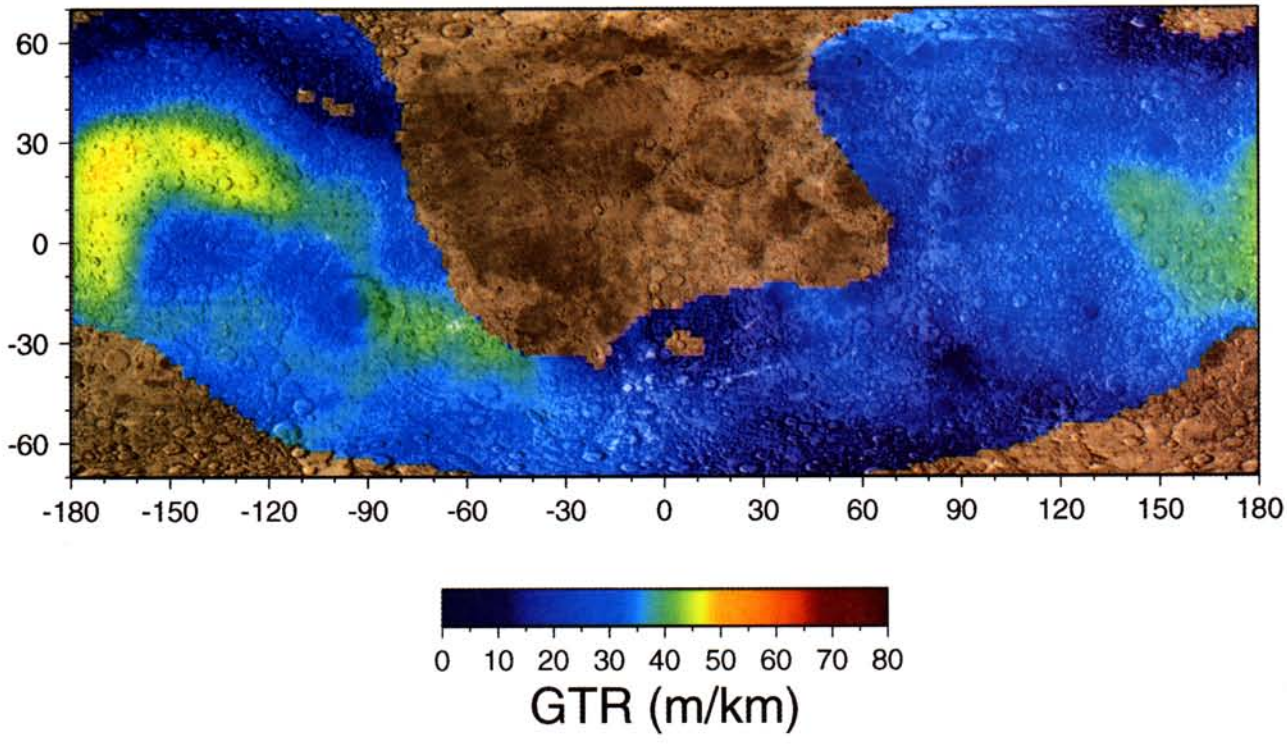

Plate 1. Map of lunar highland GTRs as determined by a linear least squares fit between the geoid and topography using data points within 1000 km radius circles.

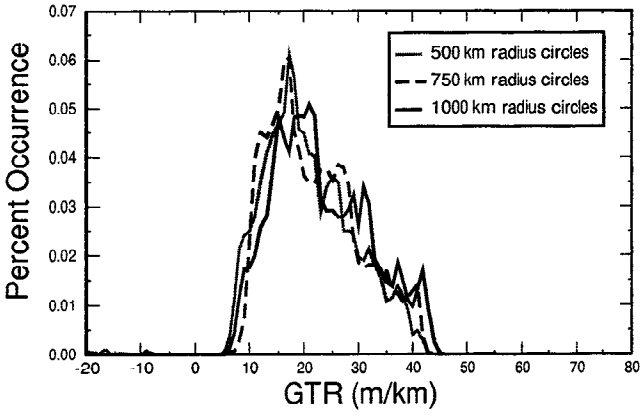

Figure 7. Histogram of GTRs for the nearside highlands using data points within 500, 750, and 1000 km radius circles.

Apollo 12/14 site, this basalt fill is only a thin veneer (less than 0.35 km [*De Hon,* 1979]) and to first order can be totally ignored. The elevation would have been slightly lower before the basalts were emplaced, but using the present elevation (−1.5 km) will only slightly overestimate the model crustal thickness at this site. Since the degree 1 topography may be due partially to hemispheric density variations within the crust, as an end-member we also determine the model crustal thickness at the Apollo 12/14 site using the present elevation with the degree 1 topography removed (−0.1 km).

For the Pratt model of compensation, the crustal thickness at mean planetary radius was found to be 67 ± 28 km. Although this range of values is consistent with Pratt compensation occurring at the seismically determined Moho (approximately 60 km depth), evidence for lateral density variations, as are required for the Pratt model, are not observed. Figure 8 shows that the abundance of iron with respect to elevation for the nearside highlands is relatively constant (i.e., mineralogy is not significantly correlated with elevation). The same is true for the farside highlands but the curve is shifted vertically. Using the linear relationship between iron concentration and density (Figure 5) and equation (19), the expected relationship between iron abundance and topography is also shown for a Pratt compensation model with a zero-elevation crustal thickness of 60 km. As can be seen, the slopes of these two distributions differ by more than an order of magnitude, suggesting that lateral density variations do not play any significant role in regional crustal compensation. This, however, does not exclude a global Pratt origin of the center-of-mass/center-of-figure offset.

For the single-layer isostatic Airy model (Figure 1a), it is not possible to state a priori whether the anorthositic crust is compensated at the lunar Moho or at an intracrustal density interface. For the range of permissible densities above and below the compensating surface, the zero-elevation model crustal thickness of the nearside highlands was found to be 43 ± 20 km. If we assume that the degree 1 topography is compensated by an Airy mechanism, the fact that the Apollo 12/14 site lies at an elevation of approximately −1.5 km implies that the model crustal thickness in this region can be no greater than 57 km, with a best estimate of 28 km. These values are lower than the seismically determined crustal thickness of 60 km, but are consistent with the existence of a 20–km seismic discontinuity that is compositional in nature. Thus, if the above single-layer Airy model is applicable for the Moon, this result suggests that the upper anorthositic crust is compensated intracrustally, and not at the Moho as has commonly been assumed. If, on the other hand, the degree 1 topography is entirely due to hemispheric density variations, then the results are more ambiguous. The crustal thickness at the Apollo 12/14 site is then constrained to lie between 20 and 64 km. Since it is most probable that reality lies somewhere between these two extremes, we feel that this model is most consistent with intracrustal compensation. Nevertheless, compensation occurring entirely at the Moho can not be excluded. We further note that if the crust is intracrustally compensated, the single layer Airy model says nothing about the thickness of the lower crust.

A two-layer Airy model with lower crustal thickness variations (Figure 1b) was used by *Goins et al.* [1981] to explain the Apollo 16 seismic data, specifically the presence of a 20–km discontinuity beneath both the Apollo mare and highland sites. However, given the seismically constrained total crustal thickness, the 1σ limits of the observed lunar GTR distribution are always smaller than the predicted model GTRs (see Figure 3), suggesting that this model is not applicable to the lunar highland crust. A highlands 20–km compositional discontinuity is thus not consistent with the observed GTRs and seismic constraints. It still remains possible that the Apollo 16 20–km discontinuity represents a transition from fractured to unfractured rocks. As discussed earlier though, the seismic evidence seems to argue against this interpretation. Given the tentative identification of the intracrustal boundary at this site, this is not a significant issue.

The last compensation model to be discussed is the two-layer Airy model with upper crustal thickness variations and constant thickness lower crust (Figure 1c). The obtained model upper crustal thicknesses at the Apollo 12/14 site have a significant range, and thus quantitative values are not very useful. This is due to the fact that the GTR is only weakly dependent on the upper crustal thickness for this model (see Figure 3c). Nevertheless, under the assumption that the degree 1 topography is compensated by an Airy mechanism, this model implies that the upper-lower crustal interface must be less than 53 km below the surface. The limits of this model indicate that anorthositic upper crustal material cannot account for the composition of the entire lunar crust. A compositionally distinct, more dense lower crustal unit must be present. If the degree 1 topography is compensated by a Pratt mechanism, then this model is consistent with, but does

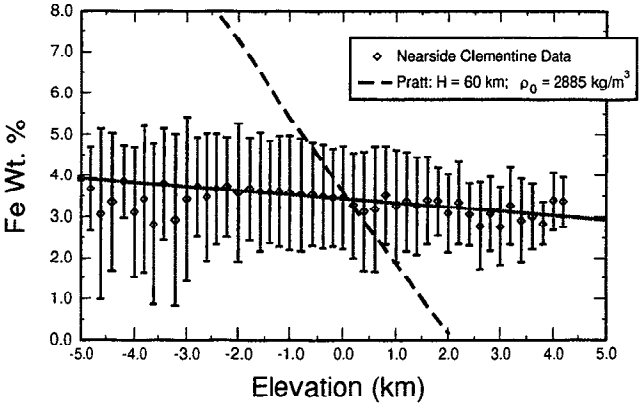

Figure 8. Plot of iron concentrations versus elevation for the lunar nearside highlands. Iron values greater than 5.5 wt % were discarded, error bars are $\pm 1\sigma$, and the degree 0 and 2 terms have been removed from the elevation data. Slope of the observed distribution is -0.099 ± 0.025 Fe wt % km^{-1}, and the slope of the expected Pratt distribution is approximately −1.77 Fe wt % km^{-1}.

Table 1. Consistency of Model Results

	Apollo 12/14 20-km Seismic Discontinuity?	Apollo 16 Tentative 20-km Seismic Discontinuity?	Apollo 12/14 60-km Seismic Discontinuity?	Apollo 16 Tentative 75-km Seismic Discontinuity?
Pratt	No	No	Yes*	Yes*
Airy	Yes*	Yes*	Yes†	Yes†
Two-layer Airy: upper crustal variations	Yes*	Yes*	Yes	Yes
Two-layer Airy: lower crustal variations	No	No	No	No

* Both cannot be true.
† In extreme cases.

not require, a stratified crust. We note that this model precludes implicitly a 20–km compositional discontinuity below both the Apollo mare and highland sites.

The results of our analysis are most consistent with the lunar crust being vertically stratified (see Table 1). Though a uniform density crust with compensation occurring at the Moho is consistent with the GTRs in extreme cases, the petrologic and seismic evidence combined with our gravity analysis strongly supports the view that the lunar crust is stratified in some manner. Indeed, if the above analysis was able to conclusively show that the crust was not stratified, many interesting questions would arise. Specifically, the existence of a 20–km seismic discontinuity below the Apollo 12/14 site, as well as the common assumption that noritic LKFM impact melt rocks represent lower crustal material would both require some form of special pleading.

This hypothesis that the crust is stratified can be further tested and improved upon in the following ways. First, the Airy isostatic admittance models that were used are relatively simple, in that they used the constraint of equal mass in vertical columns. More sophisticated admittance models can be developed that take into account membrane stresses, bending stresses, and self gravitational effects [e.g., *Turcotte et al.*, 1981; *Sleep and Phillips*, 1985]. If membrane and bending stresses are included for the single-layer Airy model, we note that our result of intracrustal compensation is further strengthened. Second, the fidelity of the gravity field used in these analyses could be explored more fully by comparing the spherical harmonic gravity inversion with line-of-sight gravity inversions over the highlands. Spectral leakage from the large mascon anomalies may have contaminated the gravity field over the highlands and may have biased the calculated GTRs (either upward or downward). And last, if it could be conclusively shown that the degree 1 topography is due to Airy crustal thickness variations, and not Pratt hemispheric density variations, then in even the most extreme cases intracrustal compensation would be required for the considered Airy compensation models. Perhaps an analysis of the composition of central peaks using Clementine spectral reflectance data could show that the farside crust is considerably thicker than the nearside crust.

Implications for Crustal Structure

Without additional seismic data, the lunar highland GTRs cannot uniquely distinguish between the single-layer Airy model and the two-layer Airy model with upper crustal thickness variations. Nonetheless, the following important results do hold.

1. Lateral variations in crustal density are more than an order of magnitude less than expected if the highland crust was exclusively compensated by a Pratt mechanism. If the surface chemistry is representative of the underlying crust, a regional Pratt component of compensation would be insignificant. Hemispheric density variations may however be important, and contribute to the lunar center-of-mass/center-of-figure offset.

2. A two-layer Airy model with lower crustal thickness variations, constant thickness upper crust, and compensation occurring at the Moho does not fit the observed lunar GTRs and whole-crust seismological constraints.

3. Both the single-layer Airy model and two-layer Airy model with upper crustal thickness variations are consistent with the lunar crust being vertically stratified. The depth of the intracrustal interface is compatible with the existence of a 20–km seismic discontinuity beneath the Apollo 12/14 site. Though a uniform density crust is compatible with the GTRs in the most extreme cases, the petrological and seismological data strongly support the crust being stratified.

4. The GTR results support the interpretation that the 20–km intracrustal seismic discontinuity is at least partially compositional in nature, and that this boundary is widespread within the lunar crust.

These results shed light on the origin of the 20–km discontinuity below the Apollo 12/14 site. We suggest that this intracrustal seismic discontinuity is both a fracture boundary as well as a compositional boundary. Furthermore, we propose that the change in composition is the reason that a fracture discontinuity does exist. A density contrast (impedance mismatch) within the crust would cause only a fraction of impact shock energy to be transmitted into the lower crust. Additionally, the more mafic lower crust should have a higher dynamic yield strength [e.g., *Melosh*, 1989]. The combination of these two factors may have inhibited, or greatly diminished, the formation of shock related microfractures below this compositional discontinuity.

The origin of the upper crustal thickness variations is enigmatic. One possibility is that these variations are due to the redistribution of surface materials by basin forming impacts. If this scenario is valid, compensation could occur at the Moho, the upper-lower crustal interface, or possibly at both locations. Where compensation would occur in this model would depend on the relative viscosities of the upper crust, lower crust, and mantle at the time of loading. It should be noted that even if surface loads were compensated entirely within the crust, nonisostatic relief on the Moho may still exist from basin forming impact events.

It is also possible that the crustal thickness variations are primordial in origin and represent the remnants of anorthositic "rockbergs" that floated in a magma ocean. If the crustal thickness variations were solely due to the redistribution of surface materials, any primordial correlation which may have existed between mineralogy and elevation would have disappeared during the formation of the lunar basins and the emplacement of their ejecta blankets. The fact that a negative correlation between thorium and elevation for the lunar highlands has been found in the Apollo data [*Metzger et al.*, 1977] suggests that it is plausible for at least some of the crustal thickness variations to be primordial in origin. Since a floating "rockberg" would be compensated at the base of the anorthositic crust, the single-layer Airy model would better describe the lunar GTRs in this scenario.

One question which this study has not addressed is the composition of the lower crust. Two plausible candidates include the LKFM impact melts and the Mg-suite norites and troctolites. The Mg-suite rocks are generally believed to have formed as intrusive lower crustal plutons after solidification of a global magma ocean [see *Warren*, 1985, for a review]. Our results suggest that a more mafic lower crust is present below the nearside highlands, and has a thickness in excess of 20 km. If the lower crustal layer is composed exclusively of Mg-suite rocks, this would seem to imply that the magmatic event that formed them was a nearly global phenomenon and that the plutons intruded the crust to a relatively uniform depth.

Impact melts having the composition of LKFM have been commonly attributed to a lower crustal origin [*Ryder and Wood*, 1977; *Charette et al.*, 1977; *Spudis et al.*, 1984; *Spudis*, 1984]. The petrologic origin of the protolith to the LKFM melt rocks, however, remains enigmatic [*Spudis et al.*, 1991]. *Hess et al.* [1977] interpreted LKFM as being "an intercumulus component in the plagioclase-rich lunar crust, and therefore a relatively primitive liquid formed during the early crystallization of the moon." Whether this primitive magma solidified to form a global LKFM crustal layer or further differentiated is not certain. In any case, the GTR results combined with the petrologic and seismic data strongly suggest that the lunar crust is stratified in some manner.

Acknowledgments. We graciously acknowledge Maria Zuber and William Kaula for reviews which greatly improved this paper. We also thank Mark Simons and Greg Neumann for reviews of an early version of this manuscript. This research was supported by NASA grants NAGW-3024 and NAGW-4881.

References

Belton, M. J. S., et al., Lunar impact basins and crustal heterogeneity: New western limb and far side data from Galileo, *Science, 255*, 570–576, 1992.

Bielefeld, M. J., R. C. Reedy, A. E. Metzger, J. I. Trombka, and J. R. Arnold, Surface chemistry of selected lunar regions, *Proc. Lunar Sci. Conf. 7th*, 2661–2676, 1976.

Bills, B. G., and F. G. Lemoine, Gravitational and topographic isotropy of the Earth, Moon, Mars, and Venus, *J. Geophys. Res., 100*, 26,275–26,295, 1995.

Bills, B. G., and D. P. Rubincam, Constraints on density models from radial moments: Applications to Earth, Moon, and Mars, *J. Geophys. Res., 100*, 26,305–26,315, 1995.

Charette, M. P., S. R. Taylor, J. B. Adams, and T. B. McCord, The detection of soils of Fra Mauro basalt and anorthositic gabbro composition in the lunar highlands by remote spectral reflectance techniques, *Proc. Lunar Sci. Conf. 8th*, 1049–1061, 1977.

De Hon, R. A., Thickness of the western mare basalts, *Proc. Lunar Planet. Sci. Conf. 10th*, 2935–2955, 1979.

Dorman, L. M., and T. R. Lewis, Experimental isostasy; 1, Theory of the determination of the Earth's isostatic response to a concentrated load, *J. Geophys. Res., 75*, 3357–3365, 1970.

Forsyth, D. W., Subsurface loading and estimates of the flexural rigidity of continental lithosphere, *J. Geophys. Res., 90*, 12,623–12,632, 1985.

Goins, N. R., A. M. Dainty, and M. N. Toksöz, Structure of the lunar crust at highland site Apollo station 16, *Geophys. Res. Lett., 8*, 29–32, 1981.

Haines, E. L., and A. E. Metzger, Lunar highland crustal models based on iron concentrations: Isostasy and center-of-mass displacement, *Proc. Lunar Planet. Sci. Conf. 11th*, 689–718, 1980.

Haxby, W. F., and D. L. Turcotte, On isostatic geoid anomalies, *J. Geophys. Res., 83*, 5473–5478, 1978.

Head, J. W., et al., Lunar impact basins: New data from the western limb and far side (Orientale and South Pole-Aitken basins) from the first Galileo flyby, *J. Geophys. Res., 98*, 17,149–17,181, 1993.

Hess, P. C., M. J. Rutherford, and H. W. Cambell, Origin and evolution of LKFM basalt, *Proc. Lunar Sci. Conf., 8th*, 2357–2373, 1977.

Hood, L. L., Geophysical constraints on the lunar interior, in *Origin of the Moon*, edited by W. K. Hartmann et al., pp. 361–410, Lunar and Planetary Inst., Houston, Tex., 1986.

Kaula, W. M., Theory of statistical analysis of data distributed over a sphere, *Rev. Geophys., 5*, 83–107, 1967.

Lambeck, K. *Geophysical Geodesy*, chap. 2, Clarendon, Oxford, England, 1988.

Lambeck, K., and S. Pullan, The lunar fossil bulge hypothesis revisited, *Phys. Earth Planet. Inter., 22*, 29–35, 1980.

Liebermann, R. C., and A. E. Ringwood, Elastic properties of anorthite and the nature of the lunar crust, *Earth Planet. Sci. Lett., 31*, 69–74, 1976.

Lingenfelter, R. E., and G. Schubert, Evidence for convection in planetary interiors from first-order topography, *Moon, 7*, 172–180, 1973.

Lucey, P. G., G. J. Taylor, and E. Malaret, Abundance and distribution of iron on the Moon, *Science, 268*, 1150–1153, 1995.

Lucey, P. G., G. J. Taylor, B. R. Hawke, and P. D. Spudis, Iron and titanium concentrations in South Pole-Aitken basin: Implications for lunar mantle composition and basin formation (abstract), *Lunar Planet. Sci. Conf., 27*, 783–784, 1996.

Melosh, H. J., Large impact craters and the moon's orientation, *Earth Planet. Sci. Lett., 26*, 353–360, 1975.

Melosh, H. J., in *Impact Cratering: A Geologic Process*, chap. 3, Oxford Univ. Press, New York, 1989.

Metzger, A. E., and R. E. Parker, The distribution of titanium on the lunar surface, *Earth Planet. Sci. Lett., 45*, 155–171, 1979.

Metzger, A. E., E. L. Haines, R. E. Parker, and R. G. Radocinski, Thorium concentrations in the lunar surface, 1; Regional values and crustal content, *Proc. Lunar Sci. Conf., 8th*, 949–999, 1977.

Mueller S., G. J. Taylor, and R. J. Phillips, Lunar composition: A geophysical and petrological synthesis, *J. Geophys. Res., 93*, 6338–6352, 1988.

Neumann, G. A., M. T. Zuber, D. E. Smith, and F. G. Lemoine, The lunar crust: Global structure and signature of major basins, *J. Geophys. Res., 101*, 16,841–16,843, 1996.

Nozette, S., et al., The Clementine mission to the Moon: Scientific overview, *Science, 266*, 1835–1839, 1994.

Ockendon, J. R., and D. L. Turcotte, On the gravitational potential and field anomalies due to thin mass layers, *Geophys. J. R. Astron. Soc., 48*, 479–492, 1977.

Pieters, C. M., et al., Crustal diversity of the Moon: Compositional analyses of Galileo solid state imaging data, *J. Geophys. Res., 98*, 17,127–17,148, 1993.

Pohl, J., D. Stöffler, H. Gall, and K. Ernstson, The Ries impact crater, in *Impact and Explosion Cratering*, edited by D. J. Roddy et al., pp. 343–404, Pergamon, New York, 1977.

Rapp, R. H., The decay of the spectrum of the gravitational potential and the topography for the Earth, *Geophys. J. Int., 99*, 449–455, 1989.

Reid, A. M., J. Warner, W. I. Ridley, and R. W. Brown, Major element compositions of glasses in the three Apollo 15 soils, *Meteoritics, 7*, 395–415, 1972.

Reid, A. M., A. R. Duncan, and S. H. Richardson, In search of LKFM, *Proc. Lunar Sci. Conf. 8th*, 2321–2338, 1977.

Ryder, G., and J. A. Wood, Serenitatis and Imbrium impact melts: Implications for large-scale layering in the lunar crust, *Proc. Lunar Sci. Conf. 8th*, 655–668, 1977.

Simmons, G., T. Todd, and H. Wang, The 25-km discontinuity: Implications for lunar history, *Science, 182*, 158–161, 1973.

Simmons, G., R. Siegfried, and D. Richter, Characteristics of microcracks in lunar samples, *Proc. Lunar Sci. Conf. 6th*, 3227–3254, 1975.

Sleep, N. H., and R. J. Phillips, Gravity and lithospheric stress on the terrestrial planets with reference to the Tharsis region of Mars, *J. Geophys. Res., 90*, 4469–4489, 1985.

Smith, D. E., M. T. Zuber, G. A. Neumann, and F. G. Lemoine, Topography of the Moon from the Clementine lidar, *J. Geophys. Res., 102*, 1591–1611, 1997.

Solomon, S. C., The nature of isostasy on the Moon: How big of a Pratt-fall for Airy models, *Proc. Lunar Planet. Sci. Conf., 9th*, 3499–3511, 1978.

Spudis, P. D., Apollo 16 site geology and impact melts: Implications for the geologic history of the lunar highlands, *Proc. Lunar Planet. Sci. Conf. 15th, Part 1, J. Geophys. Res., 89, suppl.*, C95–C107, 1984.

Spudis, P., B. R. Hawke, and P. Lucey, Composition of the Orientale basin deposits and implications for the lunar basin-forming process, *Proc. Lunar Planet. Sci. Conf. 15th, Part 1, J. Geophys. Res., 89, suppl.*, C197–C210, 1984.

Spudis, P. D., G. Ryder, G. J. Taylor, K. A. McCormick, K. Keil, and R. A. E. Grieve, Source of mineral fragments in impact melts 15445 and 15455: Toward the origin of Low-K Fra Mauro basalt, *Proc. Lunar Planet. Sci. Conf., 21st*, 151–165, 1991.

Spudis, P. D., R. A. Reisse, and J. J. Gillis, Ancient multiring basins on the Moon revealed by Clementine laser altimetry, *Science, 266*, 1848–1851, 1994.

Todd, T., D. A. Richter, G. Simmons, and H. Wang, Unique characterization of lunar samples by physical properties, *Proc. Lunar Planet. Sci. Conf., 4th*, 2639–2662, 1973.

Toksöz, M. N, A. M. Dainty, S. C. Solomon, and K. R. Anderson, Structure of the Moon, *Rev. Geophys., 12*, 539–567, 1974.

Turcotte, D. L., A fractal interpretation of topography and geoid spectra on the Earth, Moon, Venus, and Mars, *Proc. Lunar Planet. Sci. Conf. 17th, Part 2, J. Geophys. Res., 92, suppl.*, E597–E601, 1987.

Turcotte, D. L., R. J. Willemann, W. F. Haxby, and J. Norberry, Role of membrane stresses in the support of planetary topography, *J. Geophys. Res., 86*, 3951–3959, 1981.

Wang, H., T. Todd, D. Richter, and G. Simmons, Elastic properties of plagioclase aggregates and seismic velocities in the Moon, *Proc. Lunar Planet. Sci. Conf., 4th*, 2663–2671, 1973.

Warren, P. H., The magma ocean concept and lunar evolution, *Annu. Rev. Earth Planet. Sci., 13*, 201–240, 1985.

Wasson, J. T., and P. H. Warren, Contribution of the mantle to the lunar asymmetry, *Icarus, 44*, 752–771, 1980.

Zuber, M. T., T. D. Bechel, and D. W. Forsyth, Effective elastic thicknesses of the lithosphere and mechanisms of isostatic compensation in Australia, *J. Geophys. Res., 94*, 9353–9367, 1989.

Zuber, M. T., D. E. Smith, F. G. Lemoine, and G. A. Neumann, The shape and internal structure of the Moon from the Clementine mission, *Science, 266*, 1839–1843, 1994.

R. J. Phillips and M. A. Wieczorek, Department of Earth and Planetary Sciences, Washington University, Box 1169, One Brookings Drive, St. Louis, MO 63130. (e-mail: phillips@wustite.wustl.edu; markw@wurtzite.wustl.edu)

(Received October 2, 1996; revised February 25, 1997; accepted March 3, 1997.)